Progress In Electromagnetics Research, Vol. 175, 127–137, 2022

Few-Cycle Electromagnetic Pulses with Finite Energy and Bounded Angular Momentum: Analysis of the Skyrmionic Texture at Focal Plane

Luis Carretero*, Pablo Acebal, and Salvador Blaya

Abstract—Exact solutions to Maxwell equations with topological charge based on a modification to Brittingham's single cycle pulses are analyzed demonstrating that they have finite values of energy, momentum, and angular momentum. Moreover, the ratio of angular momentum to energy is bounded due to the dependence of the mean frequency on topological charge. We have also analyzed the skyrmionic texture of the electric and magnetic fields showing that it is possible to obtain skyrmionic numbers higher than the one for the magnetic field by means of a superposition of pulses with different topological charges and null skyrmionic number.

1. INTRODUCTION

For a given solution $\psi(\mathbf{r},t)$ to vacuum wave equation [1]:

$$\nabla^2\psi(\mathbf{r},t) - \frac{1}{c^2}\frac{\partial^2\psi(\mathbf{r},t)}{\partial t^2} = 0 \tag{1}$$

with c being the speed of light and ψ a complex function $\psi = \psi_R + i\,\psi_I$ ($\psi_R = \Re[\psi(\mathbf{r},t)]$ and $\psi_I = \Im[\psi(\mathbf{r},t)]$, where $\Re$ and $\Im$ are the real and imaginary parts of the function ψ), and the Hertz potential can be defined as [2, 3]:

$$\Pi_m = \mu_0\,\psi_{R,I}(\mathbf{r},t)\,\hat{z} \tag{2}$$

with μ_0 being the permeability of the vacuum. By using this potential, a TE solution to Maxwell equations is given by [2, 3]:

$$\mathbf{H}_{R,I} = \frac{\nabla\times\nabla\times\Pi_m}{\mu_0} = \left(\frac{\partial^2\psi_{R,I}}{\partial r\partial z}\hat{r} + r^{-1}\frac{\partial^2\psi_{R,I}}{\partial\varphi\partial z}\hat{\varphi} + \left(\frac{\partial^2\psi_{R,I}}{\partial z^2} - c^{-2}\frac{\partial^2\psi_{R,I}}{\partial t^2}\right)\hat{z}\right) \tag{3}$$

$$\mathbf{E}_{R,I} = -\frac{\partial}{\partial t}\nabla\times\Pi_m = \mu_0\left(-r^{-1}\frac{\partial^2\psi_{R,I}}{\partial\varphi\partial t}\hat{r} + \frac{\partial^2\psi_{R,I}}{\partial r\partial t}\hat{\varphi}\right) \tag{4}$$

where $\mathbf{E}_R$, $\mathbf{H}_R$ and $\mathbf{H}_I$, $\mathbf{E}_I$ of Equations (3) and (4) are real solutions to Maxwell equations. A TM mode can be obtained by exchanging the electric and magnetic fields.

Brittingham [4–6] proposed a function (ψ_B) that satisfies the vacuum wave Equation 1 whose solutions to Maxwell equations are spatially localized electromagnetic pulses that propagate at the speed of light:

$$\psi_B = f_{0B}\exp(-\gamma s + im\varphi)r^m(i\tau + q_1)^{-m-1} \tag{5}$$

Received 16 July 2022, Accepted 7 September 2022, Scheduled 27 September 2022

* Corresponding author: Luis Carretero (l.carretero@umh.es).

The authors are with the Óptica y Tecnología Electrónica, Dpto. de Ciencia de Materiales, Universidad Miguel Hernández, Avda. de la Universidad, 3202, Elche, Alicante, Spain.

where $s = \frac{r^2}{i\tau+q_1} - i(ct+z)$, $\tau = z - ct$, (r, φ, z) are the cylindrical coordinates; f_{0B} is a normalizing constant; m is the azimuthal index (or topological charge); and finally, γ, α, and q_1 are positive parameters.

The solutions to Maxwell equations obtained by introducing Equation (5) into Equations (2)–(4) are termed a focus wave mode (FWM) for its alleged soliton-like properties and are continuous for m integer values. They also move in a straight line and do not disperse as they propagate [5]. However, they have infinite energy [6, 2], so in order to generate solutions to the Maxwell equations with finite energy, Ziolkowsky [2] proposed using the solution to the wave equation [2, 3]:

$$\psi_Z = f_{0Z} \exp(-\gamma s)(s+q_2)^{-\alpha}(i\tau+q_1)^{-1} \tag{6}$$

where f_{0Z} and q_2 are positive parameters. Ziolkowsky's solution does not have topological charge. The electromagnetic field obtained for $\alpha = 1$ has been widely studied by many researchers including Ziolkowsky [2] and Hellwarth-Nouchi [3]. In particular, Hellwarth and Nouchi [3] demonstrated that (for $\alpha = 1$ and $\gamma = 0$) the electromagnetic field obtained has finite energy, and pulses are one-cycle or short if the imaginary part is taken and $1\frac{1}{2}$ or long if the real part is used. The singularities of these single-cycle pulses have been recently analyzed in [7]. When $\alpha \geq 1$, it is possible to obtain the family of solutions recently studied in [8] by Shen et al., which correspond to supertoroidal pulses that exhibit skyrmionic behaviour in the magnetic field. Raybould et al. have demonstrated that the electromagnetic toroidal pulses based on the Hellwarth and Nouchi solutions can be used to generate multiple Mie modes over a wide frequency region when they interact with dielectric particles [9]. Zdagkas et al. [10] have recently reported the generation of this kind of pulse by using nanostructured metasurfaces in the optical and THz region of the spectrum. On the other hand, Lekner has analyzed these types of pulses in depth [11–15] demonstrating, among many other properties, that the momentum of the pulses based on the Ziolkowsky-Nouchi function is smaller than energy/c, and that total angular momentum is null.

In this article, we are interested in studying few-cycle solutions ($\gamma = 0$) with non-null total angular momentum and finite energy. So, by comparing Equations (5) and (6) (with $m = 0$), it is easy to observe that they are the same except for the factor $(s+q_2)^{-\alpha}$, so it could be possible to obtain few-cycle solutions to Maxwell equations by using a modification (ψ_m) to the Brittingham solution including a term $(s+q_2)^{-\alpha}$. Thus, we are going to analyze the solution of the wave equation (1), ψ_m, including the term $(s+q_2)^{-\alpha}$ for the cases in which $\alpha = m+1$, $m \geq 0$:

$$\psi_m = f_m \exp(i\, m\varphi) r^m (s+q_2)^{-(m+1)} (i\tau+q_1)^{-m-1} \tag{7}$$

This expression is a solution to wave Equation (1), which then gives rise to solutions of Maxwell equations according to Equations (3) and (4). It can be observed that if $m = 0$ then Equation (7) corresponds to the Hellwarth and Nouchi single cycle solutions and to the previously cited toroidal pulses with skyrmionic magnetic fields [8]. Equation (7) represents a particular case of functions with azimuthal dependence based on the Hillion solution described by Lekner [14, 15]. Lekner has studied similar functions for different cases like the superposition of TE and TM dephased pulses or pseudo circularly polarized pulses with azimuthal dependence, analyzing the different properties of the electromagnetic field. Moreover, Ornigotti et al. have also analyzed the effect of orbital angular momentum on nondiffracting ultrashort optical pulses obtained by generalizing the X-wave solution of the Maxwell equations [16].

Thus, we are going to analyze the electromagnetic properties and skyrmionic texture for different azimuthal parameters $m \geq 1$ of the solutions to Maxwell equations obtained by introducing Equation (7) into Equations (3)–(4).

2. ELECTROMAGNETIC PROPERTIES OF THE FIELDS

For a given real electromagnetic field $\mathbf{E}$, $\mathbf{H}$ the energy u, Poynting vector $\mathbf{s}$, momentum $\mathbf{p}$, and angular momentum $\mathbf{j}$ densities are given respectively by:

$$u = \frac{1}{2}\epsilon_0|\mathbf{E}|^2 + \frac{1}{2}\mu_0|\mathbf{H}|^2, \quad \mathbf{s} = \mathbf{E}\times\mathbf{H}, \quad \mathbf{p} = \frac{\mathbf{s}}{c^2}, \quad \mathbf{j} = \mathbf{r}\times\mathbf{p} \tag{8}$$

U being the total energy, $\mathbf{J}$ angular momentum and $\mathbf{P}$ the momentum given by the volume integrals:

$$U = \int u\, d^3r, \quad \mathbf{P} = \int \mathbf{p} d^3r, \quad \mathbf{J} = \int \mathbf{j} d^3r \tag{9}$$

Figure 1 shows the energy density of the electromagnetic field at the focal region (at time $t = 0$) for the values of $m = 0$, 1, 2, and 3. As can be seen, $m = 0$ corresponds to the toroidal pulse [3, 8]. The energy distribution becomes more complex as the m parameter increases. As can be observed at time $t = 0$, only the fields $m = 0$ and $m = 1$ present energy density at the z-axis (pulse propagation direction), which in the case of $m = 0$ is purely magnetic.

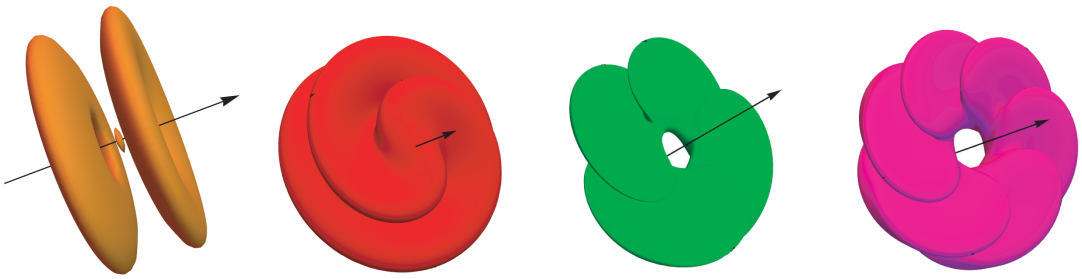

Figure 1. Isosurfaces for the energy density of the electromagnetic field at the focal region ($t = 0$) for the values of $m = 0$ (orange), $m = 1$ (red), $m = 3$ (green) and $m = 4$ (magenta). Pulse parameter: $q_1 = 20q_2$. Black vector represents the z-axis (propagation direction).

Figure 2 shows the energy densities at the focal plane $z = 0$ for the time $t = 0$ choosing different values of the topological charge m. As can be observed, only modes for $m \geq 2$ show vortex at origin. These energy densities show the same spatial distribution as the electric field lines described in [6].

The electromagnetic energy density shown in Figure 2, for topological charge $m \geq 2$, bears a resemblance to petal-like beamsthat which can be obtained when two modes with angular momentum and opposite helicity are added coherently [17, 18].

It has been recently demonstrated that the Poynting vector vanishes along the propagation axis ($r = 0$) by using the electromagnetic field associated to ψ_0 [7, 8]. This property is satisfied for all electromagnetic fields obtained by using the functions ψ_m if $m \geq 0$ except when $m = 1$, in this case:

$$\mathbf{s}_1(0, z, t) = \frac{4c\mu_0 f_1^2(-q_1^2 + q_2^2 + 4ctz)}{(q_1^2 + (-ct + z)^2)^3(q_2^2 + (ct + z)^2)^3}\hat{z} \tag{10}$$

This result is valid for both real and imaginary electromagnetic fields given in Equations (3) and (4). Assuming $q_1 \neq q_2$, it can be observed that $\mathbf{s}_1 \neq 0$ if the pulse is at focus at $t = 0$, and for all time t and position z if $z\,t \neq (q_1^2 - q_2^2)/(4c)$. So, from the electromagnetic pulses obtained by using the functions ψ_m, the only one that carries axial power is the one with topological charge 1.

If the electromagnetic field is obtained by using the functions ψ_m according to Equations (3) and (4), the magnitudes U_m, $\mathbf{P}_m$, and $\mathbf{J}_m$ are time invariant [15], so they can be obtained for $t = 0$ without any loss of generality. By introducing Equation (7) into Equations (3), (4), and (8), evaluating them at $t = 0$, and performing the integrals 9, we obtain that energy, momentum, and angular momentum for modes $m \geq 0$ are:

$$U_m = \frac{(m+2)(m+1)^2}{2^{2m+3}} \frac{\pi^2 f_m^2 \mu_0}{q_1^{m+3} q_2^{m+3}} (q_1 + q_2) \tag{11}$$

$$\mathbf{P}_m = \frac{(m+2)(m+1)^2}{2^{2m+3}} \frac{\pi^2 f_m^2 \mu_0}{c\, q_1^{m+3} q_2^{m+3}} (q_2 - q_1)\hat{z} \tag{12}$$

$$\mathbf{J}_m = -\frac{m(m+1)^2}{2^{2m+2}} \frac{\pi^2 f_m^2 \mu_0}{c\, q_1^{m+2} q_2^{m+2}} \hat{z} \tag{13}$$

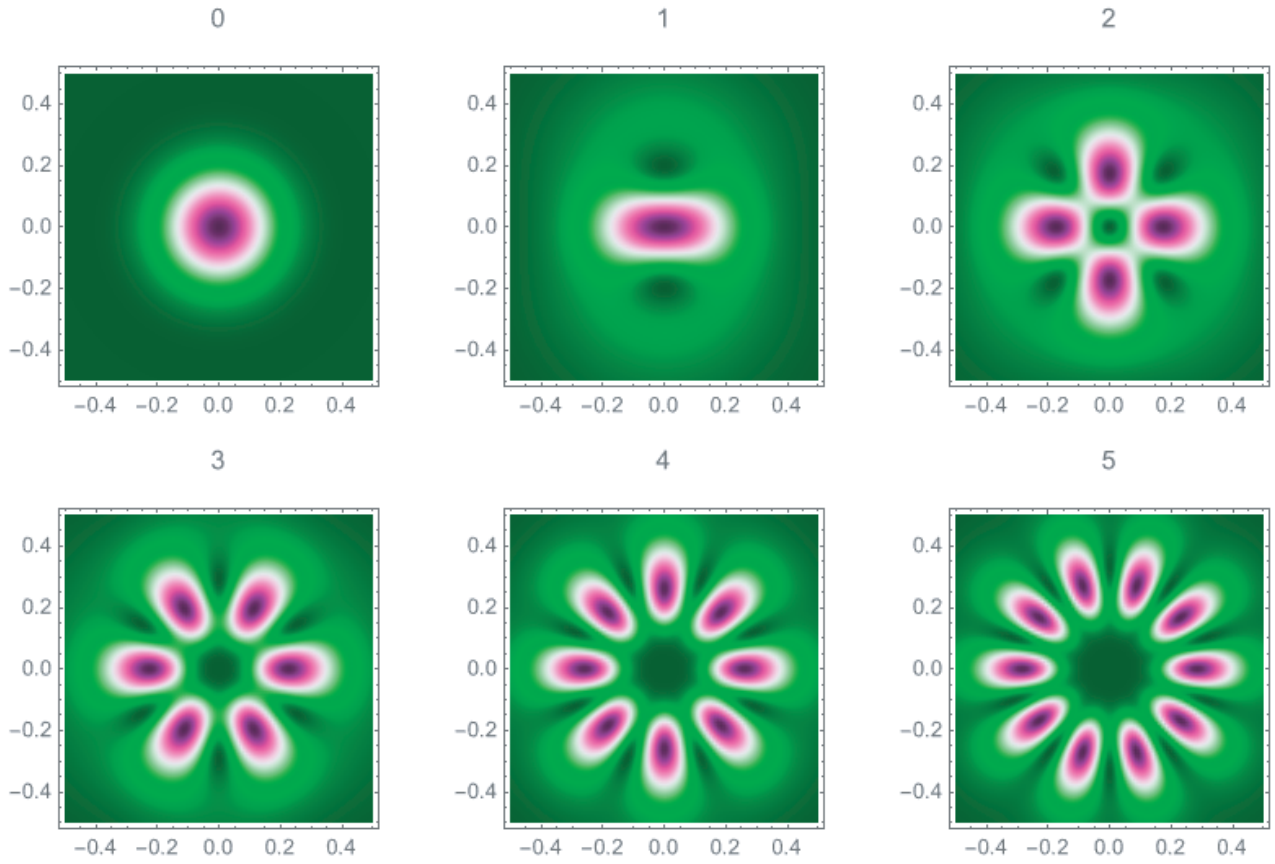

Figure 2. Electromagnetic energy density on focal plane $z = 0$ for the time $t = 0$ for the values of $m =$ 0, 1, 2, 3, 4 and 5. Dimensions of graphics are $q_2^2/4$.

Equations (11)–(13) are valid for real and imaginary fields $\mathbf{E}_{R,I}$, $\mathbf{H}_{R,I}$. Equation (11) generalizes the result obtained by Hellwarth and Nouchi [3] for $m = 0$ and demonstrates that the pulses obtained by using Brittingham's modified solution given by Equation (7) has finite energy. Momentum and angular momentum given by Equations (12) and (13) are finite too, and only present axial components with the angular momentum are directed against the propagation direction of the pulse. It can be deduced from Equation (12) that if $q_2 = q_1$, the pulse momentum is null because the forward and backward propagation terms in Equation (7) have equal weight. Moreover if $q_2 > q_1$, then the pulse propagates in the positive z direction, and the momentum is heading in that direction. It is interesting to note that according to Equations (11)–(13), all fundamental modes fulfill the conditions:

$$c\frac{P_{m,z}}{U_m} = \beta = (q_2 - q_1)/(q_1 + q_2) < 1, \forall m \tag{14}$$

$$c\frac{J_{m,z}}{U_m} = -\frac{2m}{m+2}\frac{q_1 q_2}{q_1 + q_2}, \forall m \tag{15}$$

Again, Equations (14) and (15) are valid for real and imaginary solutions. The result given by Equation 14 is independent of m, and it is the same as the one obtained by Lekner [11, 15] for single-cycle pulses with $m = 0$ and shows that the net momentum of the electromagnetic field is lower than its energy $/c$. According to Lekner, $c^2\frac{P_{m,z}}{U_m} = \beta c$ can be interpreted as an average of energy velocity, and taking into account that $\beta < 1$, there exists a Lorentz transformation to a frame L_0 in which the total momentum is zero [11, 15] for any topological charge m.

On the other hand, Equation (15) establishes that the fundamental mode for $m = 0$ does not have angular momentum in the pulse propagation direction. For $m \geq 1$, the angular momentum $J_{m,z}$ is negative, and it is directed against the propagation direction of the pulse, which implies that the TE

analyzed pulses are noncausal [15], meaning that they contain backward-propagating elements. It can also be deduced from Equation (15) that the ratio of angular momentum to energy is bounded, and it has a minimum negative value of $2q_1q_2/(c(q_1+q_2))$ obtained for large values of m. This result is related to the fundamental limit described by Ornigotti [16], to the amount of angular momentum that a single cycle optical pulse can carry, which is quite different from the one obtained, for example, with monochromatic Laguerre-Gaussian (paraxial or non paraxial) beams [19] for which $\frac{\tilde{J}_{m,z}}{\tilde{U}_m} = m/\omega$, and it is not bounded. However, in this case it is important to note that $\tilde{J}_{m,z}$ and $\tilde{U}_m$ refer to angular momentum and energy per unit of length, and are integrated over a surface at a fixed plane and not over a volume according to:

$$\frac{\tilde{J}_{m,z}}{\tilde{U}_m} = \frac{\iint r dr d\varphi j_z}{c \iint r dr d\varphi u} \tag{16}$$

We have carried out integral (16) by introducing Equation (7) into Equations (3), (4), and (8), evaluating them at plane $z = 0$ and $t = 0$, with the result being:

$$\frac{\tilde{J}_{m,z}}{\tilde{U}_m} = -\frac{(q_1+q_2)\left(2m^2q_1q_2 + 5mq_1q_2\right)}{c(m+2)\left(mq_1^2 + 2mq_1q_2 + mq_2^2 + 3q_1^2 + 4q_1q_2 + 3q_2^2\right)} \tag{17}$$

This result is valid for real and imaginary fields, and it can be deduced from Equation (17) that $\frac{\tilde{J}_{m,z}}{\tilde{U}_m}$ is bounded, being the minimum value obtained for large values of m: $-2q_1q_2/(c(q_1+q_2))$, a value that is equal to the one obtained when volumetric integrals are used.

Recently, Porras [20] has demonstrated that the azimuthal index (topological charge m) is bounded, and consequently the angular orbital momentum carried by pulses obtained by a superposition of Laguerre-Gaussian beams is bounded too. It is important to note that in our case the azimuthal number m is not bounded, but it is deduced from Equation (15) that for a finite and fixed energy U_m the angular momentum $|J_{m,z}| = \frac{2m}{m+2}\frac{q_1q_2}{q_1+q_2}\frac{U_m}{c}$ is bounded for large values of m to $2\frac{q_1q_2}{q_1+q_2}\frac{U_m}{c}$. In the next subsection, we are going to study the reason that the ratio of angular momentum to energy is bounded.

2.1. Energy Spectra and Mean Frequency of the Pulse

Applying the same methodology as Nouchi et al. [3] in Section 4 of their paper, we focus on real fields although the results are identical to those of imaginary ones. Thus, the spectrum $V_{\omega,R}$ is defined as [3]:

$$U_m = \frac{1}{2\pi}\int_0^\infty V_{\omega,R} d\omega \tag{18}$$

In order to obtain $V_{\omega,R}$, we use the relation [3]:

$$V_{\omega,R} = 2\epsilon_0 c \int_0^\pi |F_\omega(R,\theta)|^2 R^2 \sin(\theta) d\theta \tag{19}$$

where the integral is carried out over the surface of a sphere in the far field of the outward traveling pulse. $|F_\omega(R,\theta)|$ is obtained from the Fourier transform:

$$F_\omega(R,\theta) = \int_{-\infty}^\infty \exp(i\omega t)\tilde{\mathbf{E}}_R dt \tag{20}$$

$\tilde{\mathbf{E}}_R$ represents the far field approximation of the electric field given in Equation (4) obtained as the limit at large radius R [3] (note that we use the spherical coordinates ($R = \sqrt{r^2+z^2}$, $\theta = \arctan(r/z)$, φ) to obtain this limit). Equation (19) can be used to obtain the mean frequency of the pulse given by:

$$\overline{\omega} = \frac{\int_0^\infty V_\omega \omega d\omega}{\int_0^\infty V_\omega d\omega} \tag{21}$$

Using the far field approximation (ψ_a) for ψ_m [3], we obtain:

$$\psi_m \to \psi_a = \frac{(-1)^{m+1} f_m \sin(\theta)^m \exp(im\varphi)}{R\, 2^{m+1}} \frac{1}{(ct - R + iQ)^{m+1}} \tag{22}$$

where $Q = \frac{1}{2}(-(q_2 - q_1)\cos(\theta) + q_1 + q_2)$, and introducing Equation (22) into (4) (using only the azimuthal component of the field, because the contribution in the far field is higher than that of the radial component due to the factor $r^{-1} = R^{-1}\sin^{-1}(\theta)$, as can be observed in Equation (4)), we find that the azimuthal component of the real electric field is given by:

$$\tilde{\mathbf{E}}_R = \frac{1}{2}\frac{\partial^2(\psi_a + \psi_a^*)}{\partial t \partial r}\hat{\varphi} \tag{23}$$

Introducing Equation (23) into Equation (20), we obtain that:

$$F_\omega(R,\theta) = -i\omega \frac{\partial}{\partial r}\int_{-\infty}^{\infty} \frac{(\psi_a + \psi_a^*)}{2}\exp(i\omega t)dt. \tag{24}$$

So performing the integral and taking the solution for $\omega > 0$, we obtain:

$$|F_\omega(R,\theta)|^2 = \frac{\pi^2 f_m^2 \mu_0^2 \left(\frac{\omega}{c}\right)^{2(m+2)} \exp\left(-\frac{2Q\omega}{c}\right)\sin(\theta)^{2(m+1)}}{R^2 (m!)^2 2^{2m+2}} \tag{25}$$

Introducing (25) into (19) and using the software Mathematica [21] to perform the integral in Equation 19, we obtain that:

$$V_{\omega,R} = 2\frac{f_m^2 \pi^{7/2}(m+1)\mu_0 \omega^4 \left(\frac{\omega}{c}\right)^{2m} \exp\left(-\frac{\omega(q_1+q_2)}{c}\right) {}_0\tilde{F}_1\left(;m+\frac{5}{2};\frac{(q_1-q_2)^2\omega^2}{4c^2}\right)}{4^m\, c^5 m!} \tag{26}$$

with ${}_0\tilde{F}_1$ being the hypergeometric regularized function. This expression in 18 reproduces the result for the total pulse energy given in Equation (11) for any value of topological charge m. The mean frequency of the pulse can be determined by introducing Equation (26) into Equation (21):

$$\overline{\omega} = \frac{1}{2}c\left(\frac{m+3}{q_1} + \frac{m+3}{q_2} - \frac{2}{q_1+q_2}\right) \tag{27}$$

It is important to note that the mean frequency given by Equation (27) depends on the parameters q_1 and q_2 of the pulse and the topological charge m. It can be deduced from Equation (27) that the mean frequency increases with m as it rises, being a special characteristic of this kind of pulses. This result implies that pulse duration $T = 2\pi/\overline{\omega}$ decreases if the imprinted topological charge increases. Ornigotti et al. [16] have found (using a different method) that the carrier frequency is also proportional to $m+2$ for other few-cycle pulses with topological charge m, which are also exact solutions to Maxwell equations. Although there are no sustained oscillations in the pulses derived from (7) [11], we can use the effective frequency $\overline{\omega}$ in order to calculate the conventional expression [19] applied to pulses for which $\frac{c\,J_{m,z}}{U_m} = m/\overline{\omega}$ obtaining that:

$$\frac{c\,J_{m,z}}{U_m} = \frac{m}{\overline{\omega}} = \frac{2m}{c\left(\frac{m+3}{q_1} + \frac{m+3}{q_2} - \frac{2}{q_1+q_2}\right)}, \quad \text{and:} \quad \lim_{m\to\infty}\frac{c\,J_{m,z}}{U_m} = \frac{2q_1q_2}{(q_1+q_2)} \tag{28}$$

which coincides with the bounded value previously obtained for $\frac{J_{m,z}}{U_m}$, and consequently, demonstrating that the angular momentum of the pulses is bounded. The main factor for obtaining this result is the dependence of $\overline{\omega}$ on the topological charge m.

Another important magnitude is the variance of the pulse spectrum given by:

$$\sigma^2 = \frac{\int_0^\infty V_\omega(\omega - \overline{\omega})^2 d\omega}{\int_0^\infty V_\omega d\omega} = \frac{1}{4}c^2\left(\frac{m+3}{q_1^2} + \frac{m+3}{q_2^2} - \frac{4}{(q_1+q_2)^2}\right) \tag{29}$$

Porras [20] recently demonstrated that $m < \overline{\omega}^2/\sigma^2$, which implies that the angular momentum of pulses obtained by a superposition of Laguerre-Gaussian beams is bounded, as we mentioned previously. Using Equations (29) and (27) and taking into account that $q_1 > 0$, $q_2 > 0$ and $m \geq 0$ we obtain that:

$$\frac{\overline{\omega}^2}{\sigma^2} = \frac{\left((m+3)q_1^2 + 2(m+2)q_1q_2 + (m+3)q_2\right)^2}{(m+3)q_1^4 + 2(m+3)q_1^3q_2 + 2(m+1)q_1^2q_2^2 + 2(m+3)q_1q_2^3 + (m+3)q_2^4} > m \tag{30}$$

Therefore, this result proves that the inequality demonstrated by Porras [20] holds for the pulses analyzed too. However, the inequality of Equation (30), unlike what happens for the Laguerre-Gaussian beams analyzed by Porras, does not imply restriction in the values of topological charge although the angular momentum is bounded, as we have demonstrated.

3. SKYRMIONIC TEXTURE OF ELECTRIC, MAGNETIC, MOMENTUM AND ANGULAR MOMENTUM FIELDS

It has been previously mentioned that Shen et al. [8] recently demonstrated that the magnetic field associated with the Ziolkowsky solution (6) with $\gamma = 0$ and $\alpha \geq 1$ shows skyrmionic behaviour in the magnetic field at different planes. Skyrmion is a topologically protected quasiparticle with a hedgehog-like vectorial field, whose orientation gradually changes as one moves away from the skyrmion center [8]. Different electromagnetic skyrmions have been reported recently. For example, skyrmions lattices can be generated using evanescent electromagnetic fields [22], or electromagnetic skyrmions based on magnetic localized spoof plasmons (LSPs) sustained by a wisely designed space-coiling meta-structure have been described by Deng et al. [23].

We are going to analyze the skyrmionic texture of electric and magnetic fields obtained by using ψ_m, when the pulse is focused at time $t = 0$ on the plane $z = 0$. In order to do so, it is necessary to introduce the skyrmionic number [24, 8, 25]:

$$N_{sk} = \frac{1}{4\pi}\iint \mathbf{n}\cdot\left(\frac{\partial \mathbf{n}}{\partial x}\times\frac{\partial \mathbf{n}}{\partial y}\right)dxdy = \frac{1}{4\pi}\iint \mathbf{n}\cdot\left(\frac{\partial \mathbf{n}}{\partial r}\times\frac{\partial \mathbf{n}}{\partial \varphi}\right)drd\varphi \tag{31}$$

In Equation (31), $\mathbf{n}$ is a unitary vector defined in Cartesian coordinates. Taking into account that our fields are expressed in cylindrical coordinates, it is convenient to rewrite N_{sk} for a unitary vector $\mathbf{n}_c$ in cylindrical coordinates. Let $\mathbf{n}_c = n_r(r,\varphi,z,t)\hat{r} + n_\varphi(r,\varphi,z,t)\hat{\varphi} + n_z(r,\varphi,z,t)\hat{z}$ be a unitary vector field in cylindrical coordinates, which can be expressed in Cartesian coordinates (for simplicity, we do not introduce the functional dependencies of the vector field components) as:

$$\mathbf{n} = (n_r\cos(\varphi) - n_\varphi\sin(\varphi))\hat{x} + (n_r\sin(\varphi) + n_\varphi\cos(\varphi))\hat{y} + n_z\hat{z} \tag{32}$$

so introducing Equation (32) into (31) and taking into account that:

$$|\mathbf{n}|^2 = |\mathbf{n}_c|^2 = 1 = n_r^2 + n_\varphi^2 + n_z^2 \tag{33}$$

$$\frac{\partial|\mathbf{n}|^2}{\partial r} = 0, \quad \text{then if} \quad n_\varphi \neq 0 \implies \frac{\partial n_\varphi}{\partial r} = -n_\varphi^{-1}\left(n_r\frac{\partial n_r}{\partial r} + n_z\frac{\partial n_z}{\partial r}\right) \tag{34}$$

the skyrmion number can be written as:

$$N_{sk} = \frac{1}{4\pi}\int_0^{2\pi} d\varphi\int_0^{\infty}\left(-\frac{\partial n_z}{\partial r} + N_c(r,\varphi)\right)dr \tag{35}$$

where $N_c(r,\varphi) = \mathbf{n}_c\cdot(\frac{\partial \mathbf{n}_c}{\partial r}\times\frac{\partial \mathbf{n}_c}{\partial \varphi})$.

We are going to focus on the real part solutions to Maxwell equations, which can be obtained on plane $z = 0$ and time $t = 0$ by introducing Equation (7) into Equations (3) and (4), being the corresponding expressions of the real electrical and magnetic fields:

$$\mathbf{E}_R = e_m(r)\,(m\cos(m\varphi)\hat{r} - F_m(r)\sin(m\varphi)\hat{\varphi}) \tag{36}$$

$$\mathbf{H}_R = h_m(r)\,(-F_m(r)\Delta_q\sin(m\varphi)\hat{r} - m\Delta_q\cos(m\varphi)\hat{\varphi} + G_m(r)\cos(m\varphi)\hat{z}) \tag{37}$$

where $e_m(r) = \frac{\mu_0\, c\, f_m(m+1)r^m\delta_q}{r(q_{12}+r^2)^{m+2}}$, $h_m(r) = \frac{f_m(m+1)r^m}{r(q_{12}+r^2)^{m+2}}$, $\delta_q = q_1 + q_2$, $\Delta_q = q_1 - q_2$, $q_{12} = q_1q_2$, $F_m(r) = \frac{mq_{12}-4r^2-mr^2}{q_{12}+r^2}$ and $G_m(r) = \frac{4r((m+1)q_{12}-r^2)}{q_{12}+r^2}$.

3.1. Electric Field $\mathbf{E}_R$

Due to the symmetry of Equation (36), the electric field does not show skyrmionic texture on the plane $z = 0$. To prove it, let $\mathbf{n}_c = \mathbf{E}_R/|\mathbf{E}_R|$: it can be deduced from Equation (36) that $\mathbf{n}_c$ does not have an axial component; thus $\partial n_z/\partial r = 0$, and, on the other hand, $\partial \mathbf{n}_c/\partial r = \pm\cos(m\varphi)\sin(m\varphi)F'_m(r)/(mF_m(r))\partial \mathbf{n}_c/\partial\varphi$, so $\partial \mathbf{n}_c/\partial r \times \partial \mathbf{n}_c/\partial\varphi = 0$ because both vectors are parallels, so the skyrmionic number $N_{sk} = 0$. It is therefore demonstrated that the electric field does not have skyrmionic texture at the time and on the plane analyzed.

3.2. Magnetic Field $\mathbf{H}_R$

According to Equation (37), if $m = 0$, the magnetic field has only an axial component, so $\mathbf{n} = \mathbf{n}_c = \mathbf{H}_R/|\mathbf{H}_R| = n_z$. Then by Equation (31), $(\frac{\partial \mathbf{n}}{\partial r} \times \frac{\partial \mathbf{n}}{\partial \varphi}) = 0$, and we obtain that $N_{sk} = 0$.

If $m \neq 0$, it can be deduced from Equation (37) that:

$$\int_0^{2\pi} N_c(r,\varphi)d\varphi = \int_0^{2\pi} \frac{\Delta_q^2 m^2 F_m(r)G'_m(r)\cos(m\varphi)d\varphi}{\left(\Delta_q^2 F_m(r)^2\sin^2(m\varphi) + \cos^2(m\varphi)\left(G_m(r)^2 + \Delta_q^2 m^2\right)\right)^{3/2}} = 0 \tag{38}$$

for $\mathbf{n}_c = \mathbf{H}_R/|\mathbf{H}_R|$, the only contribution to the skyrmionic number can be due to the axial term of the unitary vector $\mathbf{n}_c = n_z(r,\varphi)$. According to Equation (35) and taking into account the integral (38), we obtain that:

$$N_{sk} = \frac{1}{4\pi}\int_0^{2\pi} (n_z(\infty,\varphi) - n_z(0,\varphi))d\varphi \tag{39}$$

being:

$$n_z(\infty,\varphi) = \lim_{r\to\infty} n_z(r,\varphi) \tag{40}$$

The axial component n_z can be obtained by introducing the Equation (37) into the definition $\mathbf{n}_c = \mathbf{H}_R/|\mathbf{H}_R|$, so:

$$n_z = \frac{G_m(r)\cos(m\varphi)}{\sqrt{\Delta \mathrm{q}^2 F_m(r)^2\sin^2(m\varphi) + G_m(r)^2\cos^2(m\varphi) + \Delta \mathrm{q}^2 m^2\cos^2(m\varphi)}} \tag{41}$$

Taking into account that $G_m(0) = 0$, we obtain that $n_z(0,\varphi) = 0$, and then there is no contribution to N_{sk} from the term $n_z(0,\varphi)$. Introducing the functions $F(r)$ and $G(r)$ into Equation (41), we obtain that:

$$n_z(\infty,\varphi) = -sign(\cos(m\varphi)),\ \forall\, m \geq 1 \tag{42}$$

Integrating the last equations according to Equation (39), it is obtained that the skyrmionic number $N_{sk} = 0$, $\forall m$, so the magnetic field does not have skyrmionic texture at the focal plane for any value of topological charge, although it has been shown by Shen et al. [8] that the magnetic field obtained with $m = 0$ shows skyrmionic textures at other planes $z \neq 0$.

It is interesting to note that it is possible to obtain a skyrmionic number greater than 1 [26, 27] on the plane $z = 0$ by the superposition of two magnetic fields like the one given in Equation (37) with two different azimuthal numbers that individually have a null skyrmionic number as we have demonstrated. Let $\mathbf{H}_{0n}$ be the magnetic field obtained by a superposition of pulses with topological charge 0 and n ($n > 0$):

$$\mathbf{H}_{0n} = \mathbf{H}_R|_{m=0} + \mathbf{H}_R|_{m=n} \tag{43}$$

For this magnetic field, it is not possible to obtain analytical expressions for the skyrmionic number given by Equation (31), but the integrals must be carried out numerically. If we assume, for example, that $q_2 = 20q_1$, $f_0 = 25$, $f_n = 1$ and perform integral 31, for $n \geq 1$ we obtain that the skyrmionic number is given by $N_{sk} = n + 1$.

Figure 3 shows the magnetic field on the plane $z = 0$ and time $t = 0$ for (a) $\mathbf{H}_R|_{m=2}$, without skyrmionic texture and (b) $\mathbf{H}_{02}$ which shows skyrmionic number $N_{sk} = 3$. Figures 3(c) and (d) show the topological density (which is the integrand in Cartesian coordinates of Equation (31) associated with the

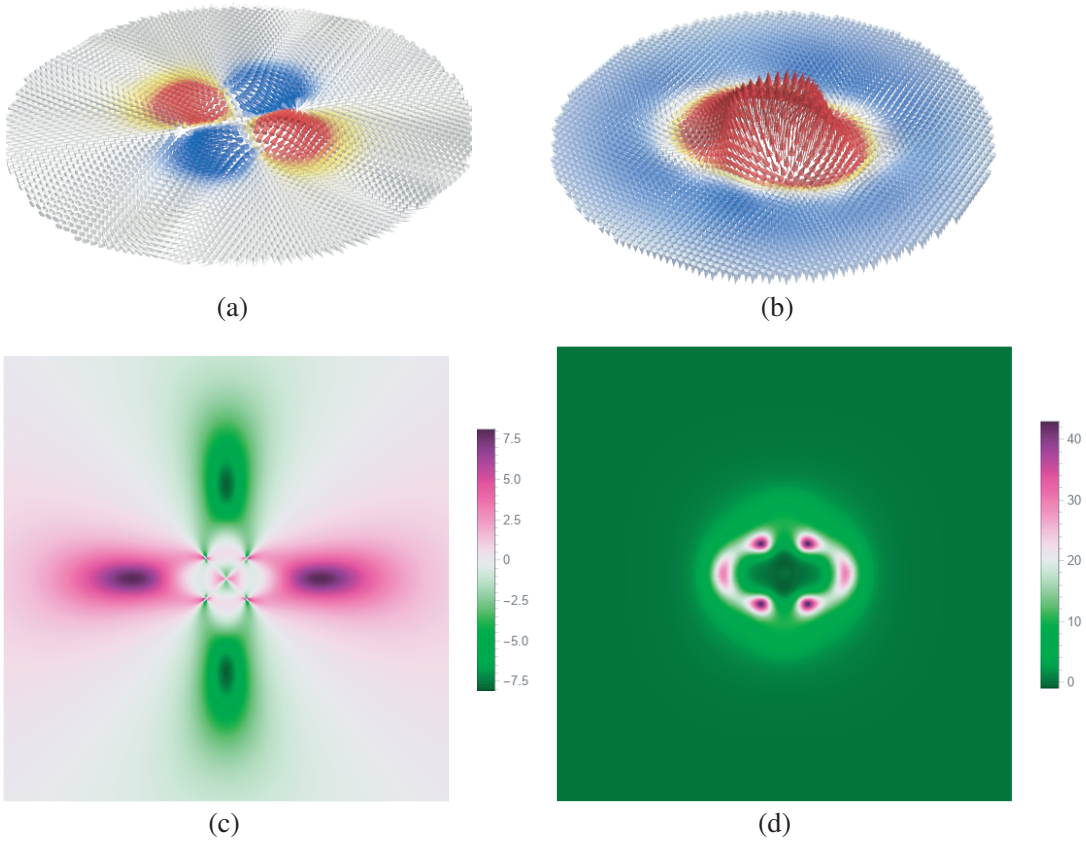

Figure 3. Magnetic fields on the plane $z = 0$ and $t = 0$ (a) $\mathbf{H}_R|_{m=2}$ without skyrmionic texture and (b) $\mathbf{H}_{02}$ that shows skyrmionic number $N_{sk} = 3$, the total surface is $q_2^2/4$. (c) Topological density associated to field (a), (d) topological density associated to the field (b). The total surface is $4q_2^2$.

magnetic fields of Figures 3(a) and (b), respectively. As can be seen, the topological density associated with $\mathbf{H}_R|_{m=2}$ is highly symmetrical showing positive and negative values, which are integrated to give rise to a null skyrmionic number. On the other hand, when we superpose to $\mathbf{H}_R|_{m=0}$ the magnetic field $\mathbf{H}_R|_{m=2}$, the topological density changes drastically, as can be observed in Figure 3(d), being highly symmetric too but positive defined, and after integration, a skyrmionic number $N_{sk} = 3$ is obtained.

4. CONCLUSION

We have analyzed the electromagnetic properties of a family of few-cycle pulses based on a modification to Brittingham's Focus Wave Mode (FWM) that are exact solution to Maxwell equations, showing that they have finite energy, momentum, and angular momentum. We have also demonstrated that, for these solutions, the mean frequency depends on the topological charge which implies that the momentum energy ratio is bounded. Finally, we have shown that it is possible to obtain a skyrmionic number greater than the one for the magnetic field by superposing a pulse without topological charge with another with topological charge that is non null. In order to obtain these results we have focused on TE electromagnetic pulses, but TM polarized pulses would create the same skyrmionic textures for the electric field.

REFERENCES

1. Born, M. and E. Wolf, *Principles of Optics: Electromagnetic Theory of Propagation, Interference and Diffraction of Light*, Cambridge University Press, 7th Edition, 1999.
2. Ziolkowski, R. W., "Localized transmission of electromagnetic energy," *Phys. Rev. A*, Vol. 39, 2005–2033, Feb. 1989.
3. Hellwarth, R. W. and P. Nouchi, "Focused one-cycle electromagnetic pulses," *Phys. Rev. E*, Vol. 54, 889–895, Jul. 1996.
4. Brittingham, J., "Focus wave modes in homogeneous Maxwell's equations — TE-mode," *1982 Antennas and Propagation Society International Symposium*, Vol. 20, 656–660, 1982.
5. Brittingham, J. N., "Focus waves modes in homogeneous Maxwell's equations: Transverse electric mode," *Journal of Applied Physics*, Vol. 54, No. 3, 1179–1189, 1983.
6. Sezginer, A., "A general formulation of focus wave modes," *Journal of Applied Physics*, Vol. 57, No. 3, 678–683, 1985.
7. Zdagkas, A., N. Papasimakis, V. Savinov, M. R. Dennis, and N. I. Zheludev, "Singularities in the flying electromagnetic doughnuts," *Nanophotonics*, Vol. 8, No. 8, 1379–1385, 2019.
8. Shen, Y., Y. Hou, N. Papasimakis, and N. I. Zheludev, "Supertoroidal light pulses as electromagnetic skyrmions propagating in free space," *Nature Communications*, Vol. 12, 5891, Oct. 2021.
9. Raybould, T., V. Fedotov, N. Papasimakis, I. Youngs, and N. Zheludev, "Focused electromagnetic doughnut pulses and their interaction with interfaces and nanostructures," *Opt. Express*, Vol. 24, 3150–3161, Feb. 2016.
10. Zdagkas, A., C. McDonnell, J. Deng, Y. Shen, G. Li, T. Ellenbogen, N. Papasimakis, and N. I. Zheludev, "Observation of toroidal pulses of light," *Nature Photonics*, Vol. 16, 523–528, Jul. 2022.
11. Lekner, J., "Electromagnetic pulses which have a zero momentum frame," *Journal of Optics A: Pure and Applied Optics*, Vol. 5, L15–L18, Apr. 2003.
12. Lekner, J., "Electromagnetic pulses, localized and causal," *Proceedings of the Royal Society A: Mathematical, Physical and Engineering Sciences*, Vol. 474, No. 2209, 20170655, 2018.
13. Lekner, J., "Angular momentum of electromagnetic pulses," *Journal of Optics A: Pure and Applied Optics*, Vol. 6, S128–S133, Feb. 2004.
14. Lekner, J., "Localized electromagnetic pulses with azimuthal dependence," *Journal of Optics A: Pure and Applied Optics*, Vol. 6, 711–716, Jun. 2004.
15. Lekner, J., *Theory of Electromagnetic Pulses*, 2053–2571, Morgan and Claypool Publishers, 2018.
16. Ornigotti, M., C. Conti, and A. Szameit, "Effect of orbital angular momentum on nondiffracting ultrashort optical pulses," *Phys. Rev. Lett.*, Vol. 115, 100401, Sep. 2015.
17. Forbes, A., "Structured light from lasers," *Laser & Photonics Reviews*, Vol. 13, No. 11, 1900140, 2019.
18. Sabatyan, A. and J. Rafighdoost, "Azimuthal phase-shifted zone plates to produce petal-like beams and ring lattice structures," *J. Opt. Soc. Am. B*, Vol. 34, 919–923, May 2017.
19. Barnett, S. M. and L. Allen, "Orbital angular momentum and nonparaxial light beams," *Optics Communications*, Vol. 110, No. 5, 670–678, 1994.
20. Porras, M. A., "Upper bound to the orbital angular momentum carried by an ultrashort pulse," *Phys. Rev. Lett.*, Vol. 122, 123904, Mar. 2019.
21. W. R. Inc., "Mathematica, Version 13.0.0." Champaign, IL, 2021.
22. Tsesses, S., E. Ostrovsky, K. Cohen, B. Gjonaj, N. H. Lindner, and G. Bartal, "Optical skyrmion lattice in evanescent electromagnetic fields," *Science*, Vol. 361, No. 6406, 993–996, 2018.
23. Deng, Z.-L., T. Shi, A. Krasnok, X. Li, and A. Alu, "Observation of localized magnetic plasmon skyrmions," *Nature Communications*, Vol. 13, 8, Jan. 2022.
24. Nagaosa, N. and Y. Tokura, "Topological properties and dynamics of magnetic skyrmions," *Nature Nanotechnology*, Vol. 8, 899–911, Dec. 2013.

25. Lin, W., Y. Ota, Y. Arakawa, and S. Iwamoto, "Microcavity-based generation of full poincaré beams with arbitrary skyrmion numbers," *Phys. Rev. Research*, Vol. 3, 023055, Apr. 2021.
26. Gergidis, L. N., V. D. Stavrou, D. Kourounis, and I. A. Panagiotopoulos, "Micromagnetic simulations study of skyrmions in magnetic FePt nanoelements," *Journal of Magnetism and Magnetic Materials*, Vol. 481, 2019.
27. Gobel, B., I. Mertig, and O. A. Tretiakov, "Beyond skyrmions: Review and perspectives of alternative magnetic quasiparticles," *Physics Reports*, Vol. 895, 1–28, 2021. Beyond skyrmions: Review and perspectives of alternative magnetic quasiparticles.